Radical Intermediates in the Reductive Isomerisation of Octahedral Manganese Carbonyl Bipyridyl Complexes; Electrochemistry, Electron Spin Resonance Spectroscopy and Molecular-orbital Calculations†

Nathan C. Brown,[a] **Gabino A. Carriedo,**[b] **Neil G. Connelly,**[a] **Francisco J. Garcia Alonso,**[b] **Ian C. Quarmby,**[a] **Anne L. Rieger,**[c] **Philip H. Rieger,**[c] **Victor Riera**[b] **and Marilin Vivanco**[b]

[a] *School of Chemistry, University of Bristol, Bristol BS8 1TS, UK*

[b] *Departamento de Quimica Organica e Inorganica, University of Oviedo, Oviedo 33071, Spain*

[c] *Department of Chemistry, Brown University, Providence, RI 02912, USA*

The complexes *fac*-[Mn(CO)$_3$L(bipy)]$^+$ [L = CNBu^t or P(OMe)$_3$, bipy = 2,2'-bipyridyl], *cis,trans*- and *cis,cis*-[Mn(CO)$_2$L(L')(bipy)]$^+$ [L = L' = CNBu^t, P(OEt)$_3$, P(OPh)$_3$ or PPh$_3$; L = CNBu^t, L' = P(OMe)$_3$], *fac*-[Mn(CO)(CNBu^t)$_3$(bipy)]$^+$ and *mer*-[Mn(CO)L$_3$(bipy)]$^+$ [L = CNBu^t or P(OR)$_3$, R = Me or Et] underwent one-electron oxidation at a platinum-disc electrode in CH$_2$Cl$_2$ and/or one-electron reduction in tetrahydrofuran (thf). The complexes *mer*-[Mn(CO)L$_3$(bipy)]$^+$ [L = P(OEt)$_3$ or CNBu^t] were oxidised by [N$_2$C$_6$H$_4$F-*p*][PF$_6$] to give dications with ESR spectra characteristic of low-spin d^5 transition-metal complexes. The ESR spectroscopic studies of the sodium amalgam reduction of *mer*- and *fac*-[Mn(CO)(CNBu^t)$_3$(bipy)]$^+$, *cis,trans*- and *cis,cis*-[Mn(CO)$_2$(CNBu^t)$_2$(bipy)]$^+$, *mer*-[Mn(CO){P-(OMe)$_3$}(bipy)]$^+$, or *cis,trans*-[Mn(CO)$_2${P(OMe)$_3$}$_2$(bipy)]$^+$ in thf provide evidence for the intermediacy of neutral bipyridyl ligand-based radicals in the reductive isomerisation of the *cis,cis* to the *cis,trans*, and of the *fac* to the *mer*, cations. Extended-Hückel molecular-orbital calculations on the *mer* and *fac* isomers of [Mn(CO)L$_3$(bipy)]$^+$ and the *cis,trans* and *cis,cis* isomers of [Mn(CO)$_2$L$_2$(bipy)]$^+$ (L = CNH or PH$_3$) provide support for the formation of metal- and ligand-based radicals on oxidation and reduction respectively.

Redox-induced isomerisation reactions are becoming increasingly common in organometallic chemistry.[1] Most are initiated by one-electron oxidation[2] though reductive processes are also known.[3] The redox isomerisation of 18-electron octahedral metal carbonyl derivatives, for example *cis*- to *trans*-[MnX-(CO)$_2$L(L–L)]^4 [X = Br or CN, L = phosphine or phosphite, L–L = Ph$_2$PCH$_2$PPh$_2$ (dppm) or Ph$_2$PCH$_2$CH$_2$PPh$_2$ (dppe)] and *cis*- to *trans*-[M(CO)$_2$(L–L)$_2$] (M = Cr, Mo or W),[5] has been invariably induced by one-electron oxidation and involves 17-electron intermediates in which the unpaired electron is largely metal-based.[6] By contrast, the reduction of metal carbonyls normally results in reactions other than isomerisation. For example, detailed studies of [Mn(CO)$_{6-n}$L$_n$]$^+$ show the primary products, *i.e.* the 19-electron radicals [Mn(CO)$_{6-n}$L$_n$], act as precursors to metal hydrides, metal formyls, binuclear species and/or derivatives of [Mn(CO)$_5$]$^-$.[7,8] The isomerisation of *cis,cis*-[Mn(CO)$_2$(CNBu^t)$_2$(L–L)]$^+$ and *fac*-[Mn(CO)-(CNBu^t)$_3$(L–L)]$^+$ [L–L = 2,2'-bipyridyl (bipy) or 1,10-phenanthroline (phen)] to the corresponding *cis,trans* and *mer* isomers on treatment with a reductant, namely sodium amalgam, and then with an oxidant, namely air, was therefore unprecedented[9] and prompted us to investigate the mechanism of these tranformations. We now report electrochemical, ESR spectroscopic, and theoretical (extended-Hückel) studies which provide evidence to support the intermediacy of metal-complexed bipyridyl anion radicals in a reductively induced isomerisation process.

Results and Discussion

The structures of the complexes used in this study, namely [Mn(CO)$_{4-n}$L$_n$(bipy)]$^+$ (*n* = 1–3), are shown in Scheme 1 together with those of the known isomers of [MnX(CO)$_2$L(L–

L)] (X = Br, CN, *etc.*) for comparison. Of the four isomers possible for a complex of general formula [MX(CO)$_2$L(bidentate ligand)] the two observed for the bipy complexes (**b** and **c**) are not the same as the two observed for the diphosphine ligands (**f** and **g**) (though **c** and **f** are equivalent).

Electrochemistry.—Oxidation. Each of the complexes *cis*, *trans*- and *cis,cis*-[Mn(CO)$_2$L(L')(bipy)]$^+$ [L = L' = CNBu^t, P(OEt)$_3$, P(OPh)$_3$ or PPh$_3$; L = CNBu^t, L' = P(OMe)$_3$], *fac*-[Mn(CO)(CNBu^t)$_3$(bipy)]$^+$ and *mer*-[Mn(CO)L$_3$(bipy)]$^+$ [L = CNBu^t or P(OR)$_3$, R = Me or Et] undergoes one-electron oxidation at a platinum-disc electrode in CH$_2$Cl$_2$ (Table 1); in most cases the process is reversible [$(i_p)_{red}/(i_p)_{ox}$ = 1.0] for scan rates v $\geqslant$ 200 mV s^{-1}. Near-reversible or fully reversible oxidation waves were also observed for *fac*-[Mn-(CO)(CNBu^t)$_3$(bipy)]$^+$ and *mer*-[Mn(CO)L$_3$(bipy)]$^+$ [L = CNBu^t or P(OMe)$_3$] in tetrahydrofuran (thf).

In CH$_2$Cl$_2$, the oxidation potential, E_{ox}, is most dependent on the degree of carbonyl substitution in [Mn(CO)$_{4-n}$L$_n$(bipy)]$^+$ so that for a given ligand L a unit increase in *n* results in a shift to more negative potential of *ca.* 0.6–0.7 V. For *n* = 1 no oxidation wave was observed but on the basis of the data for the complexes with *n* = 2 and 3 the oxidation of [Mn(CO)$_3$L-(bipy)]$^+$ can be estimated at *ca.* 1.8 V or more positive, outside the accessible range with the supporting electrolyte and solvent system used. Changes in E_{ox}, dependent on *n*, have been noted for analogous complexes of chelating ditertiary phosphines, *e.g.* [MnX(CO)$_2$L(dppm)]^2 and [MnX(CO)(dppm)$_2$]^{10} (X = Br or CN *etc.*) and for many other metal carbonyl derivatives,[11] and have usually been interpreted as evidence for metal-based oxidation.

Table 1 Electrochemical[a] data for manganese bipyridyl complexes

Complex	E_{ox}^{b}/V	$(i_p)_{red}/(i_p)_{ox}^{c}$	E_{red}^{d}/V	$(i_p)_{ox}/(i_p)_{red}$
fac-[Mn(CO)$_3$(CNBu^t)(bipy)]$^+$	e	e	-1.21	0.0
fac-[Mn(CO)$_3$\{P(OMe)$_3$\}(bipy)]$^+$	e	e	-1.24	0.0
$cis,trans$-[Mn(CO)$_2$(CNBu^t)$_2$(bipy)]$^+$	1.25	1.0	-1.36	1.0
cis,cis-[Mn(CO)$_2$(CNBu^t)$_2$(bipy)]$^+$	1.20	1.0	-1.37	0.88
			-1.54 (CH$_2$Cl$_2$)	0.0
$cis,trans$-[Mn(CO)$_2$(CNBu^t)\{P(OMe)$_3$\}(bipy)]$^+$	1.24	1.0	-1.50 (CH$_2$Cl$_2$)	0.0
cis,cis-[Mn(CO)$_2$(CNBu^t)\{P(OMe)$_3$\}(bipy)]$^+$	1.16	1.0^f	-1.50 (CH$_2$Cl$_2$)	0.0
$cis,trans$-[Mn(CO)$_2$\{P(OEt)$_3$\}$_2$(bipy)]$^+$	1.17	1.0	g	
$cis,trans$-[Mn(CO)$_2$\{P(OMe)$_3$\}$_2$(bipy)]$^+$	1.24	1.0	-1.34	0.85
			-1.55 (CH$_2$Cl$_2$)	0.0
cis,cis-[Mn(CO)$_2$\{P(OEt)$_3$\}$_2$(bipy)]$^+$	1.06	1.0	g	
$cis,trans$-[Mn(CO)$_2$\{P(OPh)$_3$\}$_2$(bipy)]$^+$	1.52	1.0	g	
cis,cis-[Mn(CO)$_2$\{P(OPh)$_3$\}$_2$(bipy)]$^+$	1.42	1.0	g	
$cis,trans$-[Mn(CO)$_2$(PPh$_3$)$_2$(bipy)]$^+$	1.10	1.0	g	
fac-[Mn(CO)(CNBu^t)$_3$(bipy)]$^+$	0.55 (thf)	0.86	-1.52	1.0
	0.52	0.81^h	-1.72 (CH$_2$Cl$_2$)	0.0
mer-[Mn(CO)(CNBu^t)$_3$(bipy)]$^+$	0.64 (thf)	0.94	-1.52	1.0
	0.62	0.93	-1.72 (CH$_2$Cl$_2$)	0.0
mer-[Mn(CO)\{P(OMe)$_3$\}$_3$(bipy)]$^+$	0.59 (thf)	1.0	-1.40	0.92
	0.55	1.0	-1.67 (CH$_2$Cl$_2$)	0.0
mer-[Mn(CO)\{P(OEt)$_3$\}$_3$(bipy)]$^+$	0.46	1.0	-1.8 (CH$_2$Cl$_2$)	0.0

[a] Cyclic voltammetry at a platinum-disc electrode. Potentials are for reversible waves unless stated otherwise; for partially reversible waves [0.0 < $(i_p)_{red}/(i_p)_{ox}$ (for oxidation) or $(i_p)_{ox}/(i_p)_{red}$ (for reduction) < 1.0] the potential quoted is the average for the oxidation and reduction peak potentials [$(E_p)_{ox}$ and $(E_p)_{red}$]; for completely irreversible waves the potential quoted is $(E_p)_{ox}$ or $(E_p)_{red}$ at a scan rate of 200 mV s^{-1}. [b] In CH$_2$Cl$_2$ unless stated otherwise. [c] At 200 mV s^{-1}. [d] In thf unless stated otherwise. [e] Not detected. [f] At scan rates of > 200 mV s^{-1}. [g] Not measured. [h] 1.0 at 1 V s^{-1}.
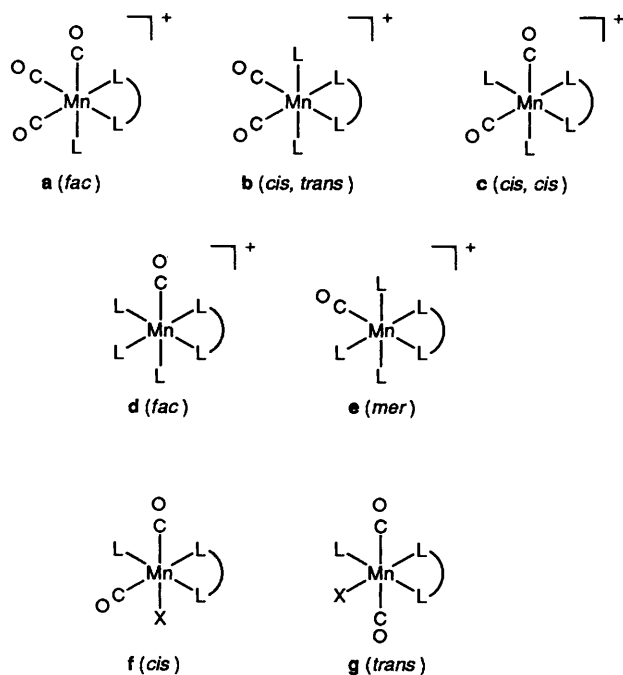
Scheme 1 In a–e L–L = bipy, in f, g L–L = ditertiary phosphine

The oxidation potential, E_{ox}, also depends on the nature of L, so that, for example, it spans a range of ca. 0.4 V (Table 1) for $cis,trans$-[Mn(CO)$_2$L(L')(bipy)]$^+$ [L = L' = CNBu^t, P(OEt)$_3$, P(OPh)$_3$, or PPh$_3$; L = CNBu^t, L' = P(OMe)$_3$]. Of more note, however, is the observation of only a minor dependence on geometry such that for a given ligand L the E_{ox} values for the $cis,trans$ and cis,cis isomers (**b** and **c**), and for the fac and mer isomers (**d** and **e**), differ by only 50–110 mV. For each pair, the isomer with two axial ligands L, namely $cis,trans$ and mer, is the more difficult to oxidise [an observation in accord with the results of molecular-orbital (MO) calculations described below].

Such a small dependence on geometry contrasts markedly with the large differences observed in E_{ox} for the cis and $trans$ isomers of species such as [M(CO)$_2$(L–L)$_2$] (M = Cr, Mo or W)[3] or [MnX(CO)$_2$L(L–L)]^2 where the cis isomer (**f**) is more difficult to oxidise than the $trans$ analogue (**g**) by ca. 0.5 V. Moreover, in these cases the cis complex is irreversibly oxidised, rapidly isomerising to the $trans$ cation after electron loss. For the complexes reported herein no evidence for oxidative isomerisation has been detected, though where the oxidation potentials of two isomers are similar, as in the case of mer- and fac-[Mo(CO)$_3$\{P(OPh)$_3$\}$_3$][12] for example, the onset of such a redox-induced transformation is not immediately obvious from simple cyclic voltammetric studies alone.

Reduction. The oxidation of the bipyridyl complexes provides an interesting comparison with analogous complexes of diphosphine ligands, particularly in the light of the ESR studies and MO calculations described below. However, the main aim of this work was to probe the mechanism of the isomerisation reactions, apparently induced by reduction, noted in the Introduction. Although cyclic voltammetry in CH$_2$Cl$_2$ showed that reduction does occur, in most cases the process was completely irreversible. Cyclic voltammetry was therefore also carried out in thf, under argon, where better defined and more informative electrochemistry was observed.

Each of the complexes fac-[Mn(CO)$_3$L(bipy)]$^+$ [L = CNBu^t or P(OMe)$_3$], $cis,trans$-[Mn(CO)$_2$(CNBu^t)$_2$(bipy)]$^+$, cis,cis-[Mn(CO)$_2$L$_2$(bipy)]$^+$ [L = CNBu^t or P(OMe)$_3$], fac-[Mn(CO)(CNBu^t)$_3$(bipy)]$^+$ and mer-[Mn(CO)L$_3$(bipy)]$^+$ [L = CNBu^t or P(OMe)$_3$] undergoes reduction at potentials in the range -1.2 to -1.5 V. In those cases where both reversible oxidation and reduction waves have been observed, $e.g.$ for fac-[Mn(CO)(CNBu^t)$_3$(bipy)]$^+$ and mer-[Mn(CO)L$_3$(bipy)]$^+$ [L = CNBu^t or P(OMe)$_3$], the wave height for the reduction process was as much as twice that for the oxidation process. Attempts to determine the number of electrons consumed during reduction by coulometry were unsuccessful, probably due to the very negative potentials required for electrolysis and the air-sensitivity of the reduction products, but the characterisation of such products by ESR spectroscopy (see below) provides good evidence for a one-electron process.

As for the oxidation reactions described above, several trends can be noted from the cyclic voltammetric data for [Mn-

$(CO)_{4-n}L_n(bipy)]^+$. First, there is a much smaller dependence of E_{red} on n such that for each additional CO ligand substituted by L the reduction wave shifts to more negative potential by only ca. 160 mV; ligand- rather than metal-based reduction is suggested. There is, however, a much more marked effect of n in that the reduction waves of the tricarbonyls fac-[Mn(CO)$_3$-L(bipy)]$^+$ [L = CNBu^t or P(OMe)$_3$], the most easily reduced of all the complexes studied, are completely irreversible; electron addition is rapidly followed by chemical reaction. These irreversible waves are accompanied by product waves which have not been further defined; similar irreversible behaviour has been observed for [Mn(CO)$_5$(PPh$_3$)]$^+$, for example, where [Mn$_2$(CO)$_8$(PPh$_3$)$_2$], [MnH(CO)$_4$(PPh$_3$)], [Mn(CO)$_5$]$^-$ and [Mn(CO)$_4$(PPh$_3$)]$^-$ were identified as products.[7]

As n increases the reversibility of the reduction wave also increases so that the di- and mono-carbonyls exhibit essentially fully reversible waves at scan rates in excess of 200 mV s^{-1}; the primary redox products, namely [Mn(CO)$_{4-n}$L$_n$(bipy)] (n = 2 or 3), are stabilised. Radicals such as [M(CO)$_{5-n}$L$_n$] (M = Mn or Re, L = phosphine, etc.) are stabilised towards dimerisation as n increases.[13,14] A similar effect may operate here in that reduction of [Mn(CO)$_{4-n}$L$_n$(bipy)]$^+$ followed by dimerisation, possibly to derivatives of [Mn$_2$(CO)$_6$(bipy)$_2$],[15] will be less favoured by increasing n.

For a given n and L, E_{red} is essentially independent of geometry, as in the case of the oxidation of the bipy compounds described above but contrasting with the oxidation of [MnX(CO)$_2$L(L–L)] (X = CN or Br, L = phosphine or phosphite, L–L = diphosphine). What little effect L has on E_{red} seems to depend on its position with respect to the bipy ligand. Thus, in the fac tricarbonyls and in the $cis,trans$ dicarbonyls, where L occupies axial sites, there is very little dependence of E_{red} on L [L = CNBu^t or P(OMe)$_3$]; in the mer monocarbonyls, with one equatorial L, there is a difference of 120 mV. However, in the light of the limited range of L available [note that the variation in E_{ox} with CNBu^t and P(OMe)$_3$ is not excessive!] such a trend should be viewed with caution.

Chemical Oxidation and Reduction.—Oxidation.

On the basis of their E_{ox} values (Table 1), the fac and mer monocarbonyls were treated with mild one-electron oxidants in the expectation that the dications fac-[Mn(CO)(CNBu^t)$_3$(bipy)]$^{2+}$ and mer-[Mn(CO)L$_3$(bipy)]$^{2+}$ [L = CNBu^t or P(OR)$_3$, R = Me or Et] might be detectable. The addition of [N$_2$C$_6$H$_4$F-p][PF$_6$] to mer-[Mn(CO){P(OR)$_3$}$_3$(bipy)]$^+$ in CH$_2$Cl$_2$ [R = Me, ν(CO) 1871 cm^{-1}; R = Et, ν(CO) 1866 cm^{-1}] resulted in a colour change from red-brown to yellow and the appearance in each case of one new carbonyl absorption [R = Me, ν(CO) 1951 cm^{-1}; R = Et, ν(CO) 1945 cm^{-1}]; the shifts to higher energy of 80 cm^{-1} are again consistent with metal-based one-electron oxidation.[14] The dications [Mn(CO){P(OR)$_3$}$_3$(bipy)]$^{2+}$ (R = Me or Et) were not isolated but the P(OEt)$_3$ complex, and the less stable dication [Mn(CO)(CNBu^t)$_3$(bipy)]$^{2+}$, were generated by in situ oxidation of the monocations and characterised at low temperature by ESR spectroscopy (see below).

Reduction. On treating the monocationic complexes in Table 1 with sodium amalgam deep purple to blue solutions were formed in thf or acetonitrile, as noted previously.[9] In some cases, treatment of suspensions of the cations in toluene with the amalgam also gives deeply coloured solutions (suggesting the formation of uncharged reduction products). Where ESR spectra were detected (see below) they were unaffected by changing the solvent (apart from variable resolution) indicating no ligand replacement even in the donor acetonitrile. It is also noteworthy that deeply coloured solutions were observed on treating [Mn(CO)$_3$L(bipy)]$^+$ [L = CNBu^t or P(OMe$_3$)] with sodium amalgam even though the cations are irreversibly reduced (Table 1) and the products are ESR silent. Though it is likely that the radicals themselves are deeply coloured the diamagnetic dimer [Mn$_2$(CO)$_6$(bipy)$_2$], possibly formed on

reduction of the less substituted cations, is violet in solution.[15]

ESR Spectra.—Reduction products.

Sodium amalgam reduction of mer- and fac-[Mn(CO)(CNBu^t)$_3$(bipy)]$^+$, $cis,trans$- and cis,cis-[Mn(CO)$_2$(CNBu^t)$_2$(bipy)]$^+$ mer-[Mn(CO){P(O-Me)$_3$}$_3$(bipy)]$^+$, or $cis,trans$-[Mn(CO)$_2${P(OMe)$_3$}$_2$(bipy)]$^+$ in thf gave stable solutions which exhibited room-temperature ESR spectra. In general the spectra were reasonably well resolved with good signal-to-noise ratio, although some variation in spectral quality was found which we attribute to small differences in sample preparation. Resolution was best at reduced temperatures, namely 220–260 K. The spectrum obtained from mer-[Mn(CO)(CNBu^t)$_3$(bipy)]$^+$ is shown in Fig. 1(a).

The appearance of the spectra is determined by small couplings to three pairs of ^{1}H nuclei [stick spectrum shown in Fig. 1(b)] and larger couplings to another pair of ^{1}H nuclei, a pair of ^{14}N nuclei, and the ^{55}Mn nucleus [stick spectrum shown in Fig. 1(c)]. When phosphite ligands are present ^{31}P couplings are observed, considerably larger than any other coupling. At the high- and low-field ends of the spectra, groups of lines are observed which permit determination of the three small couplings. Focusing on strong lines in the centre, it was possible to determine the three (or four) remaining coupling constants. The coupling constants are given in Table 2(a); assignments of the ^{1}H couplings are discussed below. In all cases, $\langle g \rangle$ = 2.0018 ± 0.0003. The ring-proton coupling constants are close to those of the bipyridyl anion radical, reported by König and Fischer,[19] Henning,[17] and Veiga et al.,[18] and those of [Mo(CO)$_{4-n}$(PBu$_3$)(bipy)]$^-$, reported by tom Dieck et al.[16]

The spectrum obtained from mer-[Mn(CO)(CNBu^t)$_3$-(bipy)]$^+$ had a very good signal-to-noise ratio, permitting least-squares fitting of the partially resolved outer groups of lines to determine the three small coupling constants and the linewidth. Best results were obtained using Gaussian line shapes; this may result from unresolved coupling, perhaps to the ^{14}N nuclei of the isocyanide ligands, but it is more likely that the Gaussian shapes reflect the fact that the pairs of protons are not exactly equivalent. If the radical were the fac isomer the ring protons should have been equivalent in pairs but in the mer isomer the nitrogen nuclei and the pairs of protons are not expected to be exactly equivalent. No extra lines are observed in the spectrum which can be attributed to this non-equivalence but the lines with $m^N = m^H = 0$ are somewhat less intense than expected when compared with the $m^N = 2$, $m^H = 1$ lines. The effect suggests a difference in coupling constants of the order of 2–3%. The spectrum obtained from the fac isomer gave coupling constants identical within experimental error to those from the mer isomer. Unfortunately, the spectrum had a poorer

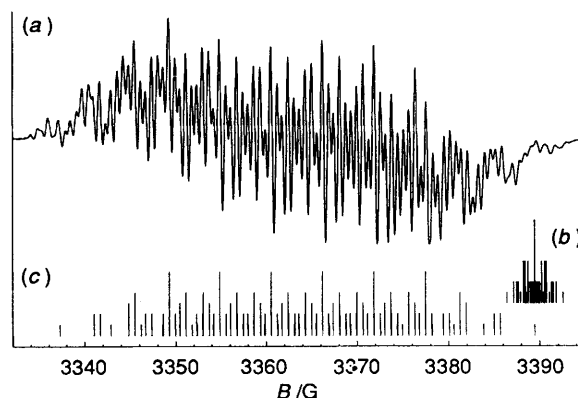Fig. 1 (a) Isotropic ESR spectrum at 220 K obtained from the sodium amalgam reduction of mer-[Mn(CO)(CNBu^t)$_3$(bipy)]$^+$ in thf. (b) Stick spectrum showing small couplings to three pairs of ^{1}H nuclei. (c) Stick spectrum showing larger couplings to two ^{1}H, two ^{14}N, and one ^{55}Mn nuclei

Table 2 ESR Parameters

(a) Reduction products[a]

Radical precursor	a_3^H	a_4^H	a_5^H	a_6^H	a^N	a^M	a^P
mer-[Mn(CO)(CNBu^t)$_3$(bipy)]$^+$	0.74	4.46	1.25	1.07	3.78	5.64	—
fac-[Mn(CO)(CNBu^t)$_3$(bipy)]$^+$	0.9	4.49	1.1	1.1	3.79	5.67	—
cis,trans-[Mn(CO)$_2$(CNBu^t)$_2$(bipy)]$^+$	0.7	4.48	1.2	1.2	3.80	5.64	—
cis,cis-[Mn(CO)$_2$(CNBu^t)$_2$(bipy)]$^+$	0.8	4.48	1.2	1.2	3.79	5.65	—
cis,trans-[Mn(CO)$_2${P(OMe)$_3$}$_2$(bipy)]$^+$	0.8	4.17	1.4	1.3	3.96	6.06	34.89[b]
mer-[Mn(CO){P(OMe)$_3$}$_3$(bipy)]$^+$	0.7	4.37	1.3	1.0	3.86	6.76	30.43[b]
[Mo(CO)$_4$(bipy)]	0.71[c]	4.2	1.23	1.04	3.6	1.7	—
fac-[Mo(CO)$_3$(PBu$_3$)(bipy)]	0.75[c]	4.2	1.1	1.1	3.55	1.8	25.5
cis,trans-[Mo(CO)$_2$(PBu$_3$)$_2$(bipy)]	0.72[c]	4.3	1.2	1.2	3.45	1.96	23.6[b]
bipy	0.54[d]	4.58	1.20	1.05	2.54	—	—
	0.61[e]	4.71	1.22	1.08	2.65	—	—
	0.58[f]	4.59	1.16	1.16	2.66	—	—

(b) Oxidation products, mer-[Mn(CO)L$_3$(bipy)]$^{2+}$

L	g_x	g_y	g_z	A_x^g	A_y^g	A_z^g	$\alpha/°$
CNBu^t	1.951(1)	2.123(6)	2.058(2)	147.3(2)	20(20)	69(1)	28(1)
P(OEt)$_3$	1.976(1)	2.139(5)	2.08(2)	135.8(5)	20(20)	20(20)	32(1)

[a] Coupling constants in G; uncertainties are ± 1 in the least significant digit. [b] Two equivalent ^{31}P nuclei. [c] Data from ref. 16. [d] Potassium complex; data from ref. 17. [e] Potassium complex; data from ref. 18. [f] Sodium complex; data from ref. 18. [g] 10^{-4} cm^{-1}.
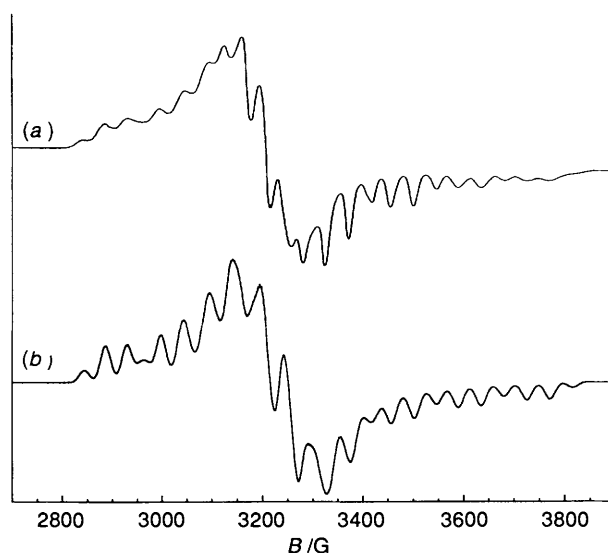

Fig. 2 The ESR spectrum of mer-[Mn(CO){P(OEt)$_3$}$_3$(bipy)]$^{2+}$ in CH$_2$Cl$_2$–C$_2$H$_4$Cl$_2$: (a) experimental at 90 K; (b) computer simulation using parameters of Table 2(b).

signal-to-noise ratio so that the fine details of line shape needed to distinguish between the mer and fac geometries are not accessible.

The spectra obtained from cis,cis- and cis,trans-[Mn(CO)$_2$(CNBu^t)$_2$(bipy)]$^+$ gave coupling constants identical within experimental error; indeed, the coupling constants are indistinguishable from those obtained from mer- and fac-[Mn(CO)(CNBu^t)$_3$(bipy)]$^+$. If the radical stereochemistry were cis,trans, the ring protons and nitrogen nuclei should have been strictly equivalent, but unfortunately the signal-to-noise ratio and resolution of the outer lines in these spectra were insufficient to determine the component line shapes or even to distinguish a_5^H and a_6^H; average values of these couplings are reported in Table 2(a).

In the spectra obtained from mer-[Mn(CO){P(OMe)$_3$}$_3$-(bipy)]$^+$ and cis,trans-[Mn(CO)$_2${P(OMe)$_3$}$_2$(bipy)]$^+$ the outer groups of lines were only partially resolved, and the signal-to-noise ratio was not sufficiently good to permit a lineshape analysis. Values of the three small coupling constants given in

Table 2(a) are thus rough estimates. Both spectra showed coupling to two equivalent ^{31}P nuclei; the centres of these spectra were complicated by second-order splitting of the central component of the phosphorus triplet by an amount comparable to the smallest ring-proton coupling. Although the stereochemistry of the radicals cannot be determined from the equivalence or non-equivalence of the ^{1}H and ^{14}N couplings, the appearance of two equivalent ^{31}P couplings argues strongly for retention of the mer and cis,trans structures. Since the unpaired electron is largely confined to a bipyridyl π* orbital, the metal contribution should be of π symmetry, an approximate d_{xz}–d_{yz} hybrid. This orbital interacts much more strongly with axial than with equatorial phosphites, so that coupling to two ^{31}P nuclei is expected for cis,trans or mer stereochemistry, but to only one ^{31}P nucleus for cis,cis or fac stereochemistry. Comparable ^{31}P couplings were observed for the axial phosphine ligands in fac-[Mo(CO)$_3$(PBu$_3$)(bipy)]$^-$ and cis,trans-[Mo(CO)$_2$(PBu$_3$)$_2$(bipy)]$^-$.[16]

Oxidation products. The bipyridyl complexes mer-[Mn-(CO)(CNBu^t)$_3$(bipy)]$^+$ and mer-[Mn(CO){P(OEt)$_3$}$_3$(bipy)]$^+$ were oxidised with [N$_2$C$_6$H$_4$F-p][PF$_6$] in CH$_2$Cl$_2$–C$_2$H$_4$Cl$_2$ (1:1). Liquid-solution spectra at or near room temperature were unresolved and, because of the asymmetric envelope, the g values could not be determined reliably. The frozen-solution spectra are qualitatively similar to those of complexes such as [Mn(CN)(CO)(dppm)$_2$]$^+$,[6,10] and analysis followed the same procedures employed in our previous work.[6]

The spectrum of [Mn(CO){P(OEt)$_3$}$_3$(bipy)]$^{2+}$ is shown in Fig. 2(a). The 'parallel' features, 1:3:3:1 quartets corresponding to hyperfine coupling to three equivalent ^{31}P nuclei (a = 45.5 G), are unevenly spaced, suggesting non-coincidence of the g and hyperfine-matrix principal axes. Given an estimate of A_y, the positions of two low-field and four high-field 'parallel' components can be fitted to afford g_x, g_y, A_x, and α (the Euler angle describing the rotation of the hyperfine-matrix x and y axes relative to the g-matrix axes). No features were found which could be reliably assigned to z components. Simulations did not lead to further refinement of the 'perpendicular' part of the spectrum so that the values of g_z, A_y and A_z given in Table 2(b) are rough estimates. A computer-simulated spectrum based on these parameters is shown in Fig. 2(b).

The spectrum of [Mn(CO)(CNBu^t)$_3$(bipy)]$^{2+}$ was poorly resolved and further complicated by weak lines assignable to a high-spin manganese(II) complex. The 'parallel' features were again unevenly spaced, suggesting non-coincidence of the g and

hyperfine-matrix principal axes. These features could be fitted, given an assumed value of A_y, to yield g_x, g_y, A_x and α. Reasonably well defined features were found which could be assigned to orientations along the z axis, but simulations were relatively insensitive to assumed values of A_y; this parameter can only be crudely estimated. Parameters are listed in Table 2(b).

The ^{31}P coupling is comparable to that observed for manganese(II) species such as $[Mn(CN)(CO)(dppm)_2]^+$, where the odd electron occupies a $d_{x^2-y^2}$ orbital with lobes 45° away from the Mn–P bonds.[6] The similar coupling, and the fact that the three ^{31}P nuclei are equivalent (within the resolution of the spectrum), suggests a similar arrangement of the three phosphite ligands with respect to the singly occupied molecular orbital (SOMO), presumably one of the t_{2g} orbitals, d_{xy}, d_{xz} or d_{yz}. This is only possible if *mer* stereochemistry is retained on one-electron oxidation and (taking the z axis as normal to the bipyridyl plane) the SOMO is predominantly d_{yz} or d_{xz}. The very similar ESR parameters suggest a similar SOMO for *mer*-$[Mn(CO)(CNBu^t)_3(bipy)]^{2+}$.

Interpretation of ESR parameters for the oxidation products. The g matrices are characteristic of low-spin d^5 metal complexes with one component less than g_e and two components larger than g_e. In our previous work[6,20] we have shown that, if the principal metal contribution to the SOMO is one of the t_{2g} set, d_{xy}, d_{xz} or d_{yz}, with a small admixture of another of the t_{2g} orbitals, the ^{55}Mn hyperfine matrix components can be related to the 3d spin density by equation (1),[20] where $P(=$

$$A_x - \langle A \rangle = P\left[-\frac{4}{7}(c_1^2 + c_2^2) + \frac{2}{3}\Delta g_x + \frac{5}{42}(\Delta g_y + \Delta g_z) \right] \quad (1)$$

207.6×10^{-4} cm^{-1}) is the dipolar constant for manganese,[21] $\Delta g_i = g_i - g_e$ and c_1 and c_2 are the LCAO (linear combination of atomic orbitals) coefficients of the major and minor contributions, assumed here to be d_{yz} and d_{xz}, respectively. The d-electron spin density is the sum of these coefficients squared, $\rho^d = c_1^2 + c_2^2$. Using the parameters given in Table 2(b), we have $\rho^d = 0.62 \pm 0.06$ and 0.66 ± 0.08 for *mer*-$[Mn(CO)(CNBu^t)_3(bipy)]^{2+}$ and *mer*-$[Mn(CO)\{P(OEt)_3\}_3(bipy)]^{2+}$, respectively. The non-coincidence angle α was found[6,20] to have approximately equal and opposite contributions, $\alpha = \alpha_A - \alpha_g \approx 2\alpha_A$, from the g and hyperfine matrices [equation (2)]. Thus the observed non-coincidence angles lead to

$$\tan 2\alpha_A = \frac{2c_2/c_1}{1 - (c_2/c_1)^2} \quad (2)$$

hybridisation ratios, $(c_2/c_1)^2 = 0.062 \pm 0.002$ and 0.082 ± 0.002 for *mer*-$[Mn(CO)(CNBu^t)_3(bipy)]^{2+}$ and *mer*-$[Mn(CO)\{P(OEt)_3\}_3(bipy)]^{2+}$, respectively.

Extended-Hückel Molecular Orbital (EHMO) Calculations.— Calculations were performed for bipy, *cis,cis*-and *cis,trans*-$[Mn(CO)_2L_2(bipy)]^+$, and *mer*- and *fac*-$[Mn(CO)L_3(bipy)]^+$ (L = CNH or PH$_3$). All C–C and C–N bond lengths in bipy were 1.40 Å except that of the 2,2′ C–C bond which was taken as 1.48 Å. Except for the N–Mn–N angle, which was 88.7°, all L–Mn–L′ bond angles were 90°. Other bond lengths were based on the crystal structure[9] of *mer*-$[Mn(CO)(CNBu^t)_3(bipy)]^+$, with Mn–P 2.395, Mn–C(CO) 1.81, Mn–C(NR) 1.92, Mn–N 2.058, C–O 1.151 and C–N 1.012 Å. The molecular axes were chosen with z normal to the bipy plane and the bipy moiety centred in the positive xy quadrant. For the *mer* complexes the three equivalent ligands were in the yz plane; for the *cis,cis* complexes the equatorial carbonyl group was along the x axis. The calculations used CAChe extended-Hückel parameters, given in Table 3, with STO-3G Gaussian functions and $K = 1.75$.[22] The standard parameters include phosphorus d orbitals, but eliminating these orbitals had a negligible effect on the calculations. The results are summarised in Table 4. Calcul-

Table 3 Extended-Hückel MO parameters

Orbital	H_{ii}/eV	ζ	Orbital	H_{ii}/eV	ζ
H 1s	13.606	1.2			
C 2s	16.59	1.576	C 2p	11.26	1.453
N 2s	20.33	1.885	N 2p	14.53	1.728
O 2s	28.48	2.192	O 2p	13.62	2.018
P 3s	16.15	1.816	P 3p	10.49	1.478
Mn 4s	7.434	1.344	Mn 4p	4.884	1.113

Orbital	H_{ii}/eV	ζ_1	ζ_2	c_1	c_2
P 3d	2.11	1.731	—	1.0	0.0
Mn 3d	9.0	5.76 739	2.509 69	0.389 84	0.729 65

ations were also done with parameters recommended by Alvarez[23] with somewhat less satisfactory results. The principal differences were substantially smaller metal participation in the LUMO (lowest unoccupied molecular orbital) (*ca.* 1%) and failure to predict hybridisation of the t_{2g} orbitals in some of the doubly occupied MOs.

Energies. For all eight model complexes the LUMO is largely identical ($\geqslant 75\%$) to the bipyridyl LUMO, and accordingly the energy varies only slightly with ligands or conformation. Thus the reduction potentials of isomeric pairs are expected to be very similar, as observed. The three highest-energy doubly occupied MOs are essentially the Mn t_{2g} set (d_{xy}, d_{xz} and d_{yz}). Their energies are determined primarily by the degree of delocalisation of a t_{2g} orgital into carbonyl and (to a lesser extent) isocyanide π^* orbitals. Thus, for example, in *mer*-$[Mn(CO)(PH_3)_3(bipy)]^+$ the d_{xz} and d_{xy} orbitals were stabilised by π interaction with CO, leaving d_{yz} as the HOMO (highest occupied molecular orbit). Similar qualitative arguments suffice to explain d_{xy} as the HOMO for *cis,cis*-$[Mn(CO)_2(CNH)_2(bipy)]^+$ and *fac*-$[Mn(CO)(CNH)_3(bipy)]^+$ and a degenerate d_{xz}–d_{yz} pair for the HOMO of *cis,trans*-$[Mn(CO)_2(PH_3)_2(bipy)]^+$, but the ordering is less obvious for the other model complexes. In particular, the HOMO for *mer*-$[Mn(CO)(CNH)_3(bipy)]^+$ depends on the relative π acidity of CO and CNH: d_{xz} interacts with CO and the axial isocyanides (and is clearly lowest in energy), d_{yz} interacts with all three isocyanides, and d_{xy} interacts with CO and the equatorial isocyanide. If the isocyanide π acidity is more than half that of CO (as in the EHMO parameterisation), d_{xy} is the HOMO; otherwise, the order is reversed. Regardless of this ambiguity, the HOMO is at higher energy for the *fac* and *cis,cis* isomers than for the corresponding *mer* and *cis,trans* complexes, consistent with the observed higher oxidation potentials for the latter isomers.

The total energy depends on the conformation, largely through variations in the energies of the t_{2g} orbitals. For the PH$_3$ model complexes the *mer* and *cis,trans* isomers are about 0.6 eV more stable than are the corresponding *fac* and *cis,cis* complexes. The difference is much smaller for the isocyanide complexes with the *mer* and *cis,trans* isomers being only marginally more stable. Since the LUMO energies are nearly constant, these predictions also apply to the neutral radicals. For the dications the *mer* and *cis,trans* phosphites remain lower in energy, but the *fac* and *cis,cis* isocyanides are now favoured.

Assignment of ring-proton couplings. In earlier work on [bipy]$^-$,[16–18] the largest ring-proton coupling was assigned to H^5, by analogy with the bipyridyl anion and on the basis of simple Hückel[17,18] or CNDO[16] (complete neglect of differential overlap) MO calculations. This work preceded the observation of the ESR spectrum of the pyridine anion in 1967 by Talcott and Myers.[24] In the pyridine anion the '*para*-directing' effect is unusually large with ring-proton couplings (G) as shown in **I**. If we regard the biphenyl anion as the superposition of two independent pyridine moieties, each with half an electron, we might expect ^1H coupling constants (G) as in **II**. On the other hand, an electron-withdrawing 2-(2′-pyridyl)

Table 4 Composition and energies of the HOMO and LUMO orbitals

Atomic orbital	*mer*	*fac*	*cis,cis*	*cis,trans*
(a) [Mn(CO)(CNH)$_3$(bipy)]$^+$ and [Mn(CO)$_2$(CNH)$_2$(bipy)]$^+$				
N 2p$_z$	0.091, 0.093	0.094	0.094, 0.095	0.093
C^2 2p$_z$	0.131, 0.134	0.134	0.134, 0.136	0.134
C^3 2p$_z$	0.026, 0.025	0.026	0.027, 0.026	0.026
C^4 2p$_z$	0.076, 0.079	0.078	0.077, 0.080	0.079
C^5 2p$_z$	0.088, 0.086	0.089	0.090, 0.089	0.088
C^6 2p$_z$	0.019, 0.022	0.020	0.020, 0.022	0.021
Mn d$_{xz}$–d$_{yz}$	0.099	0.087	0.078	0.085
LUMO, % bipy	87.0	88.2	88.9	88.2
LUMO Energy/eV	−8.68	−8.67	−8.68	−8.68
HOMO % Mn	72.6 d$_{xy}$ 0.4 d$_{z^2}$	83.8 d$_{xy}$	72.6 d$_{xy}$ 0.4 d$_{z^2}$	62.6 d$_{xy}$ 0.8 d$_{z^2}$
HOMO Energy/eV	−9.37	−9.22	−9.37	−9.52
(b) [Mn(CO)(PH$_3$)$_3$(bipy)]$^+$ and [Mn(CO)$_2$(PH$_3$)$_2$(bipy)]$^+$				
N 2p$_z$	0.077, 0.080	0.086	0.087, 0.090	0.081
C^2 2p$_z$	0.114, 0.118	0.126	0.127, 0.130	0.119
C^3 2p$_z$	0.026, 0.023	0.026	0.028, 0.025	0.025
C^4 2p$_z$	0.061, 0.066	0.071	0.070, 0.075	0.066
C^5 2p$_z$	0.081, 0.079	0.086	0.088, 0.086	0.082
C^6 2p$_z$	0.012, 0.016	0.016	0.015, 0.019	0.014
Mn d$_{xz}$–d$_{yz}$	0.218	0.144	0.122	0.190
LUMO % bipy	75.2	82.2	84.0	77.4
LUMO Energy/eV	−8.63	−8.65	−8.66	−8.64
HOMO % Mn	80.1 d$_{yz}$ 6.7 d$_{xz}$	98.7 d$_{xy}$	80.5 d$_{xy}$ 2.4 d$_{yz}$	36.2 d$_{yz}$ 36.2 d$_{xz}$
HOMO Energy/eV	−9.07	−8.96	−9.18	−9.31*

* Degenerate pair.
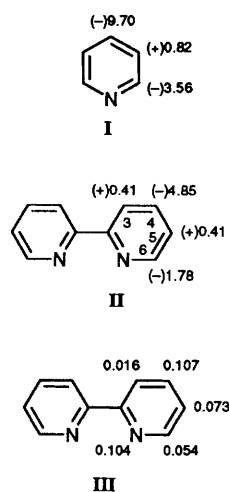
group would be expected to lead to larger (more negative) couplings for H^3 and H^5 and smaller (less negative) couplings for H^4 and H^6.

Extended-Hückel spin densities for the bipyridyl anion given in **III** are consistent with the qualitative argument given above, although coupling constants computed using the relationship[25] (3) are in only fair agreement with experiment. The predicted

$$a^H = -23.7 \, \rho_C^\pi \tag{3}$$

values of a_5^H and a_6^H are too large in magnitude and a_4^H and a_3^H are substantially too small. This can be rationalised in part by spin-polarisation effects: positions of high spin density (N, C^2 and C^4) tend to polarise adjacent positions of low spin density (C^3, C^5 and C^6) leading to larger spin densities at the former and smaller (or negative) spin densities at the latter positions. In the end we assigned ring-proton couplings in accordance with the

EHMO predictions, but with the understanding that a_3^H and a_6^H may well be reversed.

Compared with spin densities in the bipyridyl anion, calculated spin densities in the manganese complexes (Table 4) are smaller at all ring positions except C^3 and C^5. We find that a_3^H is indeed larger and a_4^H smaller, but a_5^H and a_6^H are about the same. The EHMO calculations give spin densities of 0.076 and 0.079 for the 4 and 4′ positions in *mer*-[Mn(CO)-(CNH)$_3$(bipy)], in satisfactory agreement with the 2–3% difference in these coupling constants estimated for *mer*-[Mn(CO)(CNBu^t)$_3$(bipy)].

Distinguishing between isomers. One of the aims of the EHMO calculations was to evaluate the ability of ESR spectra to distinguish between different isomers. Comparing the experimental results of Table 2(a) with the calculations summarised in Table 4(a), it is clear that if we cannot distinguish between *mer*-[Mn(CO)(CNBu^t)$_3$(bipy)] and *cis,trans*-[Mn(CO)$_2$(CNBu^t)$_2$(bipy)] on the basis of ESR coupling constants, we almost certainly could not distinguish between the *fac* and *mer* or *cis,cis* and *cis,trans* isomers. On the other hand, the isomeric forms of the phosphite complexes almost certainly could be distinguished. It is unfortunate that *cis,cis*-[Mn(CO)$_2${P(OMe)$_3$}$_3$(bipy)]$^+$ and *fac*-[Mn(CO){P(OMe)$_3$}$_3$-(bipy)]$^+$ were not available for ESR study.

Spin-density distributions in the manganese(II) species. For *mer*-[Mn(CO)(PH$_3$)$_3$(bipy)]$^+$ the HOMO [the SOMO for the manganese(II) dication] is predicted to contain about 80% Mn d$_{yz}$ and 7% d$_{xz}$ character ($R = 0.084$) with most of the remaining contributions coming from bipy orbitals. Although the predicted spin density is rather high, the hybridisation ratio is in excellent agreement with the analysis of the ESR spectrum. Furthermore, the dominant d$_{yz}$ character is consistent with the observation of equivalent hyperfine coupling to the three ^{31}P nuclei. For *mer*-[Mn(CO)(CNH)$_3$(bipy)]$^+$ the HOMO is predicted to contain 73% Mn d$_{xy}$ character with smaller contributions from equatorial carbonyl and isocyanide orbitals. This is inconsistent with the requirement of significant d hybridisation, but the next filled MO, 0.12 eV lower in energy, is

a d_{yz}–d_{xz} hybrid qualitatively consistent with the ESR result. As noted above, the order of these two orbitals depends on the relative π acidities of CO and CNBu^t; the experimental results suggest that the π acidity of CNBu^t is less than half that of CO.

Experimental

Many of the complexes used in this work are light- and air-sensitive, particularly in solution. All of the studies reported were therefore made with freshly crystallised, analytically pure (C, H and N elemental analyses) samples. All of the complexes described have been made previously, and fully characterised as [ClO$_4$]$^-$ salts.[9,26,27] In this work [PF$_6$]$^-$ salts have been used, prepared either by simple modifications of the published procedures, for cis,trans-[Mn(CO)$_2${P(OMe)$_3$}$_2$(bipy)]$^+$ and mer-[Mn(CO){P(OMe)$_3$}$_3$(bipy)]$^+$,[27] or as detailed below.

Infrared spectra were recorded on a Nicolet 5ZDX FT spectrometer. Cyclic voltammetry was carried out using an EG & G model 273 potentiostat in conjunction with a three-electrode cell. The auxiliary electrode was a platinum wire and the working electrode a platinum disc. The reference was an aqueous saturated calomel electrode (SCE) separated from the test solution by a fine-porosity frit and an agar bridge saturated with KCl. Solutions were 0.1×10^{-3} mol dm^{-3} in the test compound and 0.1 mol dm^{-3} in [NBu$_4$][PF$_6$] as the supporting electrolyte and were shielded from light using aluminium foil and from air by using a nitrogen (CH$_2$Cl$_2$) or argon (thf) atmosphere. At the end of each experiment, [Fe(η-C$_5$H$_5$)$_2$], [Fe(η-C$_5$Me$_5$)$_2$], or [Co(η-C$_5$H$_5$)$_2$]$^+$ was added to the solution as an internal standard for potential measurements. Under the conditions used the E^0 values for the couples were as follows: [Fe(η-C$_5$H$_5$)$_2$]$^+$–[Fe(η-C$_5$H$_5$)$_2$] (0.47 V, CH$_2$Cl$_2$; 0.54 V, thf); [Fe(η-C$_5$Me$_5$)$_2$]$^+$–[Fe(η-C$_5$Me$_5$)$_2$] (−0.09 V, CH$_2$Cl$_2$; 0.09 V, thf) and [Co(η-C$_5$H$_5$)$_2$]$^+$–[Co(η-C$_5$H$_5$)$_2$] (−0.84 V, thf).

Reductions for ESR spectroscopic studies were carried out by exposing the monocationic complexes in thf to a 0.5% sodium amalgam; the resulting blue to purple solutions were then transferred under argon to an ESR tube using an air-tight syringe. Oxidations were carried out by weighing stoichiometric amounts (1:1) of the manganese complex and [N$_2$C$_6$H$_4$F-p][PF$_6$] into an ESR tube. The tube and contents were de-gassed, deoxygenated CH$_2$Cl$_2$–C$_2$H$_4$Cl$_2$ (1:1) was added, and the mixture was then briefly shaken and frozen at 77 K. The ESR spectra were recorded on a Bruker ESP-300E spectro-meter, equipped with a Bruker variable-temperature accessory and a Hewlett-Packard 5350B microwave frequency counter. The field calibration was checked by measuring the resonance of the diphenylpicrylhydrazyl (dpph) radical before each series of spectra.

fac-(2,2'-Bipyridyl)(tert-butyl isocyanide)tricarbonylman-ganese Hexafluorophosphate, fac-[Mn(CO)$_3$(CNBu^t)(bipy)]-[PF$_6$].—A solution of fac-[Mn(CO)$_3$(CNBu^t)(bipy)][ClO$_4$]^{21} (0.30 g, 0.57 mmol) and [NH$_4$][PF$_6$] (1.0 g, 6.13 mmol) in CH$_2$Cl$_2$ (40 cm^3) was stirred overnight. The solution was then filtered and evaporated to dryness to yield the complex as a yellow solid, yield 0.30 g (91%). The absence of [ClO$_4$]$^-$ should be checked by IR spectroscopy in the solid state; it shows a very strong absorption at 1100 cm^{-1}.

cis,cis-(2,2'-Bipyridyl)bis(tert-butyl isocyanide)dicarbonyl-manganese Hexafluorophosphate, cis,cis-[Mn(CO)$_2$(CNBu^t)$_2$-(bipy)][PF$_6$].—A mixture of fac-[Mn(CO)$_3$(CNBu^t)(bipy)]-[PF$_6$] (400 mg, 0.76 mmol), ONMe$_3$ (63 mg, 0.84 mmol) and CNBu^t (0.095 cm^3, 0.84 mmol) in CH$_2$Cl$_2$ (40 cm^3) was stirred at room temperature for 1 h. After removing the solvent in vacuo the residue was washed with light petroleum (b.p. 60–80 °C, 3 × 15 cm^3) and then recrystallised from CH$_2$Cl$_2$–ethanol to give the product as red crystals, yield 353 mg (80%).

cis,trans-(2,2'-Bipyridyl)bis(tert-butyl isocyanide)dicarbonyl-manganase Hexafluorophosphate, cis,trans-[Mn(CO)$_2$(CN-

Bu^t)$_2$(bipy)][PF$_6$].—A solution of cis,cis-[Mn(CO)$_2$(CNBu^t)$_2$-(bipy)][PF$_6$] (200 mg, 0.34 mmol) in MeCN (25 cm^3) was stirred with 0.5% sodium amalgam (8.63 g, 1.88 mmol of Na) for 10 min at room temperature. The blue solution was then filtered in air through Celite and the resulting orange solution evaporated to dryness. The residue was washed with light petroleum (b.p. 60–80 °C, 5 × 15 cm^3) and then recrystallised from CH$_2$Cl$_2$–diethyl ether to give the product as orange crystals, yield 116 mg (58%).

fac-(2,2'-Bipyridyl)tris(tert-butyl isocyanide)carbonylmanga-nese Hexafluorophosphate, fac-[Mn(CO)(CNBu^t)$_3$(bipy)]-[PF$_6$].—A mixture of fac-[Mn(CO)$_3$(CNBu^t)(bipy)][PF$_6$] (400 mg, 0.76 mmol), ONMe$_3$ (120 mg, 1.60 mmol) and CNBu^t (0.181 cm^3, 1.60 mmol) in CH$_2$Cl$_2$ (70 cm^3) was heated under reflux for 4 h. After removing the solvent in vacuo the residue was washed with light petroleum (b.p. 60–80 °C, 5 × 15 cm^3) and then recrystallised from CH$_2$Cl$_2$–ethanol to give the product as dark red crystals, yield 358 mg (74%).

mer-(2,2'-Bipyridyl)tris(tert-butyl isocyanide)carbonyl-manganese Hexafluorophosphate, mer-[Mn(CO)(CNBu^t)$_3$-(bipy)][PF$_6$].—A solution of fac-[Mn(CO)(CNBu^t)$_3$(bipy)]-[PF$_6$] (200 mg, 0.31 mmol) in MeCN (25 cm^3) was stirred with 0.5% sodium amalgam (14.25 g, 3.10 mmol of Na) for 15 min at room temperature. The green solution was then filtered in air through Celite and the resulting red solution evaporated to dryness. The residue was washed with light petroleum (b.p. 60–80 °C, 5 × 15 cm^3) and then recrystallised from CH$_2$Cl$_2$–diethyl ether to give the product as dark red crystals, yield 128 mg (64%).

References

1 See, for example, W. E. Geiger, Prog. Inorg. Chem., 1985, 33, 275; J. K. Kochi, J. Organomet. Chem. Library, 1990, 22, 201 and refs. therein.

2 R. D. Rieke, H. Kojima, T. Saji, P. Rechberger and K. Ofele, Organometallics, 1988, 7, 749; R. H. Philp, jun., D. L. Reger and A. M. Bond, Organometallics, 1989, 8, 1714; D. J. Kuchynka and J. K. Kochi, Organometallics, 1989, 8, 677; N. G. Connelly, A. G. Orpen, A. L. Rieger, P. H. Rieger, C. J. Scott and G. M. Rosair, J. Chem. Soc., Chem. Commun., 1992, 1293.

3 C. P. Casey, L. D. Albin, M. C. Saeman and D. H. Evans, J. Organomet. Chem., 1978, 155, C37; D. J. Kuchynka and J. K. Kochi, Inorg. Chem., 1988, 27, 2574; O. B. Ryan, M. Tilset and V. D. Parker, J. Am. Chem. Soc., 1990, 112, 2618; J. M. Mevs, T. Gennett and W. E. Geiger, Organometallics, 1991, 10, 1229; K.-T. Smith and M. Tilset, J. Organomet. Chem., 1992, 431, 55; T. Roth and W. Kaim, Inorg. Chem., 1992, 31, 1930; W. E. Geiger, P. H. Rieger, C. Corbato, J. Edwin, E. Fonseca, G. A. Lane and J. M. Mevs, J. Am. Chem. Soc., 1993, 115, 2314.

4 N. G. Connelly, K. A. Hassard, B. J. Dunne, A. G. Orpen, S. J. Raven, G. A. Carriedo and V. Riera, J. Chem. Soc., Dalton Trans., 1988, 1623.

5 A. Vallat, M. Person, L. Roullier and E. Laviron, Inorg. Chem., 1987, 26, 332; A. M. Bond, B. S. Grabaric and J. J. Jackowski, Inorg. Chem., 1978, 17, 2153 and refs. therein; C. M. Elson, Inorg. Chem., 1976, 15, 469.

6 G. A. Carriedo, N. G. Connelly, E. Perez-Carreno, A. G. Orpen, A. L. Rieger, P. H. Rieger, V. Riera and G. M. Rosair, J. Chem. Soc., Dalton Trans., 1993, 3103.

7 D. J. Kuchynka, C. Amatore and J. K. Kochi, Inorg. Chem., 1986, 25, 4087.

8 B. A. Narayanan, C. Amatore and J. K. Kochi, Organometallics, 1987, 6, 129.

9 F. J. Garcia Alonso, V. Riera, M. L. Valin, D. Moreiras, M. Vivanco and X. Solans, J. Organomet. Chem., 1987, 326, C71.

10 G. A. Carriedo, V. Riera, N. G. Connelly and S. J. Raven, J. Chem. Soc., Dalton Trans., 1987, 1769.

11 R. H. Morris, K. A. Earl, R. L. Luck, N. J. Lazarowych and A. Sella, *Inorg. Chem.*, 1987, **26**, 2674; A. B. P. Lever, *Inorg. Chem.*, 1990, **29**, 1271; B. E. Bursten, *J. Am. Chem. Soc.*, 1982, **104**, 1299 and refs. therein.

12 A. M. Bond, S. W. Carr and R. Colton, *Organometallics*, 1984, **3**, 541.

13 G. B. Rattinger, R. L. Belford, H. Walker and T. L. Brown, *Inorg. Chem.*, 1989, **28**, 1059; D. J. Kuchynka, C. Amatore and J. K. Kochi, *J. Organomet. Chem.*, 1987, **328**, 133.

14 M. C. Baird, *Chem. Rev.*, 1988, **88**, 1217 and refs. therein.

15 W. Hieber, W. Beck and G. Zeitler, *Angew. Chem.*, 1961, **73**, 364.

16 H. tom Dieck, K.-D. Franz and F. Hohmann, *Chem. Ber.*, 1975, **108**, 163.

17 J. C. M. Henning, *J. Chem. Phys.*, 1966, **44**, 2139.

18 J. dos Santos Veiga, W. L. Reynolds and J. R. Bolton, *J. Chem. Phys.*, 1966, **44**, 2214.

19 V. E. König and H. Fischer, *Z. Naturforsch.*, 1962, 1063.

20 P. H. Rieger, *Coord. Chem. Rev.*, in the press; G. B. Carpenter,

G. S. Clark, A. L. Rieger, P. H. Rieger and D. A. Sweigart, *J. Chem. Soc., Dalton Trans.*, 1994, 2903.

21 J. R. Morton and K. F. Preston, *J. Magn. Reson.*, 1978, **30**, 577.

22 Personal CAChe system, CAChe Scientific inc, Beaverton, OR, 1992.

23 S. Alvarez, *Tables of Parameters for Extended Hückel Calculations*, University of Barcelona, June 1989.

24 C. L. Talcott and R. J. Myers, *Mol. Phys.*, 1967, **12**, 549.

25 M. Karplus and G. K. Fraenkel, *J. Chem. Phys.*, 1961, **35**, 1312.

26 F. J. Garcia Alonso, V. Riera, F. Villafane and M. Vivanco, *J. Organomet. Chem.*, 1984, **276**, 39.

27 G. A. Carriedo, J. Gimeno, M. Laguna and V. Riera, *J. Organomet. Chem.*, 1981, **219**, 61.